1

2

Biomass-cover relationship for eelgrass meadows

4

5 Jacob Carstensen[1*], Dorte Krause-Jensen[2], Thorsten J. S. Balsby[2]

6

7 [1] Department of Bioscience, Aarhus University, Frederiksborgvej 399, DK-4000

8 Roskilde, Denmark

9 [2]Department of Bioscience, Aarhus University, Vejlsøvej 25, DK-8600 Silkeborg,

10 Denmark

11 * corresponding author: jac@dmu.dk; Phone: +45 87158596; Fax: +45 87155010

12

15

16

17

Abstract

Eelgrass meadows play key roles in coastal ecosystems and the extent of the standing biomass is focal to

address ecosystem functioning. Eelgrass cover is commonly assessed in marine monitoring programs while

biomass sampling is destructive and expensive. Therefore, we have proposed a functional relationship that

translates eelgrass cover into aboveground biomass using site-specific information on Secchi depth or light

attenuation. The relationship was estimated by non-linear regression on 791 combined observations of

eelgrass cover and biomass from eight different coastal sites in Denmark. Eelgrass biomass initially

increased with cover and flattened out as cover exceeded 40-50% due to increased self-shading. Decreasing

light energy with depth reduced the eelgrass biomass potential (assessed at 100% cover), and this reduction

was stronger for coastal sites with lower water transparency. Moreover, the biomass potential varied

seasonally from around 110-140 g DW m^{-2} in spring months to a peak of 241 g DW m^{-2} in August, consistent

with other seasonal studies. The model explained 56% of the variation in log-transformed biomasses, but

significant variation between coastal sites still remained, deviating between -23% and 39% from the mean

relationship. These site-specific deviations could be due to differences in losses related to grazing, drifting

algae and epiphytes, better light capture by dense canopies, as well as differences in how well light

conditions within eelgrass meadows are represented by actual measurements of Secchi depth and light

attenuation. The relationship can be employed to estimate eelgrass biomass of entire coastal ecosystems from

observations of eelgrass cover and depth.

36

INTRODUCTION

Eelgrass meadows play key functional roles in coastal ecosystems because eelgrass is an engineering species capable of modifying the benthic habitat structurally and metabolically (Gutierrez et al. 2011; Hemminga and Duarte 2000). The meadows increase the structural complexity of the seafloor and provide habitat for a variety of species, thereby stimulating biodiversity (Plummer et al. 2013). They are also highly productive and hence support secondary production and have a major effect on nutrient and carbon cycling in the coastal zone. In some areas eelgrass constitutes an important food source for birds (Clausen et al. 2012), but overall few species graze directly on eelgrass, and most of the biomass enters the detrivore food web or is buried (Cebrián et al. 1997). Moreover, eelgrass meadows dissipate wave energy and stabilize the sediments within and surrounding the meadows, which help protect the coast from erosion. The reduced wave energy further promotes particles trapping, and thereby contributes to increased water clarity as well as carbon sequestration in eelgrass sediments (van der Heide et al. 2011; McGlathery et al. 2012; Duarte et al. 2013). Seagrass sediments have indeed been identified as globally important carbon stocks (Fourqurean et al. 2012). These eelgrass-mediated ecosystem services depend on the standing biomass and the area cover of the meadows, which are, therefore, key variables to address in monitoring and management of coastal ecosystems.

Mosaics of eelgrass patches and meadows occur on soft/sandy bottom of relatively protected waters from the shore and as deep as light levels allow, with the meadows confined to shallow depth ranges in turbid waters and extending deeper in clear waters (Duarte et al. 2007). The abundance of eelgrass typically declines exponentially with depth paralleling the extinction of light (Duarte 1991; Krause-Jensen et al. 2000). Physical exposure may reduce the abundance in shallow water, resulting in a bell-shaped distribution with depth (Krause-Jensen et al. 2003), and poor sediment quality or reduced oxygen levels may also lead to reduced eelgrass abundance (Koch 2001; Krause-Jensen et al. 2011). As the meadows respond to changing water and sediment quality, their distribution and abundance are often used as indicators of ecological status (Marbà et al. 2013).

63 Biomass expressed as dry weight of carbon per m^2 seafloor is a relevant unit for quantifying eelgrass

64 abundance and estimating structural and functional roles of the plant. Carbon biomass can also be quantified

65 for other ecosystem components, which potentially allows addressing carbon flow through the ecosystem via

66 coupling to process rates. But direct determination of biomass is destructive and resource-demanding as it

67 requires harvesting the plants by divers and many biomass samples would be required to determine the large-

68 scale eelgrass abundance. Eelgrass cover, assessed by divers, underwater video or remote sensing, is an

69 alternative, non-destructive variable that is less costly compared to measuring biomass and suitable for

70 assessment of eelgrass distribution and abundance at larger spatial scale. However, assessments of eelgrass

71 cover do not couple as directly to ecosystem functions as biomass observations do. The combined benefit of

72 non-destructive, large-scale and low-cost cover assessments and detailed biomass information relating more

73 directly to ecological functions, could be obtained if robust relationships between coverage observations and

74 biomass could be established to predict biomass distribution from coverage. For instance, observations of

75 eelgrass cover along depth gradients from the shore and to the deepest extension of the meadows could be

76 converted to biomass on the basis of such biomass-cover relationships. This would allow scaling cover to

77 biomass over larger areas and potentially assessing eelgrass functions at an ecosystem scale.

78

79 Here we establish and test a generic relationship between eelgrass biomass and cover, taking into account

80 factors such as depth, water clarity and time of the year. The relationship is developed based on monitoring

81 data from the Danish coastal waters with combined information on eelgrass cover and biomass along depth

82 gradients. The relationship allows the conversion of estimates of eelgrass cover to biomass along depth

83 gradients. We thereby provide the basis for obtaining estimates of eelgrass biomass based on large-scale and

84 long-term data sets on eelgrass cover. This opportunity is of great value e.g. in Denmark where the majority

85 of monitoring data on eelgrass distribution and abundance is available solely as cover estimates.

86

87

MATERIALS AND METHODS

89　Eelgrass cover has been monitored routinely since 1989 in ~50 different estuaries and coastal embayments

90　(referred to as coastal sites in the following) within the Danish National Aquatic Monitoring and Assessment

91　Program (DNAMAP). In addition to the regular eelgrass monitoring, data on the aboveground biomass of

92　eelgrass were available from specific surveys in eight coastal sites which form the study areas of the current

93　study (Table 1; Fig. S1). These data were extracted from the national marine monitoring database or from

94　reports, in cases when data had not been submitted to the database. Eelgrass biomass was sampled between

95　1990 and 2009.

96

97　Eelgrass biomass and cover were sampled in the growth season (March to October) by regional monitoring

98　authorities with support from consultants. Sampling was carried out according to the same general protocol

99　by experienced divers that regularly participate in intercalibration exercises as part of the monitoring

100　program. Biomass samples were obtained by harvesting the aboveground biomass within a frame placed

101　randomly within the eelgrass meadows where these covered the seafloor. The frame size varied between

102　coastal sites from 0.09 to 0.25 m^2 and the number of samples per depth transect ranged between 1 and 24.

103　The samples were dried at 105 °C (in few cases at 85 °C) for 24 h to constant weight and the biomass

104　reported in g dry weight (DW) m^{-2}. Before harvesting the biomass, the diver estimated the eelgrass cover

105　within the frame in percent of the soft/sandy seafloor and recorded sampling depth. We quality-controlled

106　the data by contacting the regional monitoring team and consulting monitoring reports to check that biomass

107　estimates were correctly adjusted to varying frame sizes and represented aboveground biomass per m^2. Data

108　not conforming to the quality check were discarded. The resulting data set consisted of 852 combined

109　biomass-cover observations distributed across eight coastal sites over the period 1990-2009 (Table 1).

110

111　The depth distribution of eelgrass biomass depends on the prevalent light conditions, and therefore seasonal

112　means (March to September) of Secchi depth (Z_{SD}) for the different coastal sites and years with eelgrass data

were calculated. Secchi depths were measured in all eight coastal sites as part of the DNAMAP; although not

within the eelgrass meadows but at stations in the deeper part of the coastal site. In these shallow coastal

sites the Secchi disk was occasionally visible at the bottom (censored data) and therefore censored data

regression was employed (Carstensen 2010). Secchi depth means (March-September) were estimated for

each year in all coastal sites and combined with the eelgrass biomass data, except for Kertinge Nor and

Helnæs Bugt where Secchi depth observations were too few in the year (1996) with eelgrass biomass data

and a Secchi depth mean over multiple surrounding years was calculated instead. Additionally, the light

attenuation coefficient (K_d) has been estimated from underwater PAR (photosynthetically active radiation)

profiles as part of DNAMAP in more recent years (Pedersen et al. 2014), which only partially overlap the

biomass samples in time as opposed to Secchi depth, which has been monitored regularly as part of

DNAMAP. Mean values of the product between K_d and Z_{SD} for the eight different sites were calculated for

comparison with the biomass model described below.

Eelgrass biomass model

The area-specific eelgrass biomass ($B(C,Z)$) essentially depends on the density and size of eelgrass shoots,

which is reflected in eelgrass cover ($C(Z)$). Eelgrass growth and, hence to a large extent, biomass and cover

mainly depends on the light energy reaching the eelgrass (Sand-Jensen and Borum 1991; Krause-Jensen et

al. 2000), and this is a function of the depth of the sample (Z) as well as the attenuation of light in the water

column, expressed by the light attenuation coefficient (K_d) which can be approximated from the Secchi depth

(Z_{SD}) (see below). Eelgrass biomass varies dynamically as a function of growth and loss processes, but we

assumed that the balance between eelgrass growth and respiration can be described by a seasonal model with

a depth component accounting for the reduced growth with lower light, whereas other loss processes than

respiration, such as grazing and physical destruction, and shading by drifting macroalgae are unrelated to

light and assumed to be reflected directly by the biomass and cover estimates. Hence, the model describes

steady-state conditions for eelgrass biomass in each month (March-October). The relationship between

eelgrass biomass and eelgrass cover, depth, and Secchi depth is derived step-by-step in the following.

140   We assumed that eelgrass biomass is related to eelgrass cover through a saturation-type of response,

141   displaying almost proportionality at low eelgrass coverage (no competition for light) but levelling off at

142   increasing cover due to increased competition for light. This can be formulated as:

143    $B(C, Z) = B_{max}(Z) \cdot (1 - \exp\left(-\frac{C(Z)}{k_C}\right))$ Eq. (1)

144   where $B_{max}(Z)$ is the maximum attainable biomass at a given depth, and k_c is a parameter describing how fast

145   the relationship between biomass and cover levels off. Eelgrass biomass will approach $B_{max}(Z)$ as $C(Z)$

146   increases towards 100%.

147

148   The maximum biomass as a function of depth, $B_{max}(Z)$, depends on the light-regulated reduction of biomass

149   with depth, assuming that a certain light level can sustain a certain biomass (steady-state assumption). The

150   effect of light-limited growth can be modeled using a simple hyperbolic tangent function (Platt and Jassby

151   1976)

152    $B_{max}(Z) = B_{max} \cdot \tanh(\frac{I(Z)}{I_{sat}})$ Eq. (2)

153   where B_{max} is the maximum attainable biomass when there is no light limitation, $I(Z)$ is the irradiance at

154   depth Z, and I_{sat} is a parameter equal to the irradiance level yielding 76 % of B_{max} (i.e. tanh(1)=0.76). Using

155   Lambert-Beer's law with K_d describing the light attenuation with depth the expression becomes

156    $B_{max}(Z) = B_{max} \cdot \tanh\left(\frac{I_0}{I_{sat}} \cdot \exp(-K_d \cdot Z)\right)$ Eq. (3)

157

158   Assuming that the Secchi depth (Z_{SD}) represents 20 % (see discussion) of the surface irradiance (i.e.

159    $K_d = \frac{-\log(0.2)}{Z_{SD}}$) the maximum eelgrass biomass becomes a function of Z_{SD}

160    $B_{max}(Z) = B_{max} \cdot \tanh\left(\frac{I_0}{I_{sat}} \cdot \exp\left(\log(0.2) \cdot \frac{Z}{Z_{SD}}\right)\right)$ Eq. (4)

161

162   Thus, combining Equations (1) and (4) the eelgrass biomass can be formulated as function of coverage,

163   Secchi depth and depth as:

164 $$B(C, Z) = B_{max} \cdot \tanh\left(\frac{I_0}{I_{sat}} \cdot \exp\left(\log(0.2) \cdot \frac{Z}{Z_{SD}}\right)\right) \cdot \left(1 - \exp\left(-\frac{C(Z)}{k_C}\right)\right)$$ Eq. (5)

165 Measurements of eelgrass biomass typically have a right-skewed distribution with variation between

166 replicate samples increasing with the mean. For analyzing measured biomasses it is therefore more relevant

167 to consider the log-transform of the biomass

168 $$\log(B(C, Z)) = \log(B_{max}) + \log\left(\tanh\left(\frac{I_0}{I_{sat}} \cdot \exp\left(\log(0.2) \cdot \frac{Z}{Z_{SD}}\right)\right)\right) + \log\left(1 - \exp\left(-\frac{C(Z)}{k_C}\right)\right)$$ Eq. (6)

169 Eelgrass biomass accumulates during months when production exceeds respiration, which results in a

170 seasonal effect on biomass in addition to the direct effect of light attenuation in the water column. This

171 seasonal variation describing the balance between growth and respiration was modeled by estimating the

172 parameter B_{max} specific to each month with biomass observations.

173

174 This non-linear model was fitted using the combined data set of eelgrass biomass, cover and Secchi depth by

175 means of non-linear maximum likelihood regression (PROC MODEL in SAS 9.3; SAS Institute, Cary, NC).

176 Model parameters were k_c and I_0/I_{sat} (describing the relative amount of surface radiation where light reduces

177 growth by 24%) as well as eight month-specific parameters for B_{max}. The non-linear estimation routine

178 iteratively found the optimal parameter estimates by ordinary least squares estimation. The eelgrass model

179 was tested by examining the distribution of the residuals, plotting them versus depth and cover and analyzing

180 their differences among coastal sites. The nature of the depth and cover relationships was assessed by

181 plotting the marginal relationships of eelgrass biomass versus the two predictors (cover and depth), i.e.

182 calculating eelgrass biomass adjusted for the predicted effect of cover and depth as well as interannual

183 variations in Secchi depth. Finally, the applicability of the model was tested by applying the estimated

184 relationship to four different transects, where cover and depth had been recorded.

185

186

187

188

189

RESULTS

191   The combined data set (791 observations) represented a broad span of depths (0.7-7.8 m), Secchi depths

192   (2.2-8.7 m), eelgrass cover (1-100%), and eelgrass biomass (0.2-573 g DW m^{-2}) (Table 1). Although there

193   were differences in sampling efforts across the 8 coastal sites, the data set appeared reasonably balanced and

194   not biased towards a single coastal site. All of the eight different months (March-October) used to describe

195   the seasonal variation in B_{max} were sampled at least at two coastal sites.

196   Eelgrass biomass varied over three orders of magnitude with an overall tendency to decline at depths >2 m

197   (Fig. 1a). For observations representing full (100%) eelgrass cover, the biomass varied from 26 to 546 g DW

198   m^{-2}, while the highest biomass observation was actually measured for a cover of 85%. Eelgrass cover

199   spanned broadly across the entire depth range (Fig. 1b), which allowed for estimating the eelgrass biomass

200   dependency on depth and cover with small risk of correlated parameter estimates, particularly k_c and $I_0/I_{sat.}$

201   Eelgrass biomass increased with cover across different depth strata in a similar manner, showing an initial

202   increase in biomass at low eelgrass cover before flattening when the cover exceeded 40-50% (Fig. 2).

203   Examining the data and the residuals generated from Eq. (6), two observations were identified as outliers

204   (Fig. 2); both having eelgrass biomass above 100 g DW m^{-2} at a low cover of 1% and 10%. These

205   observations were subsequently excluded from the model estimation.

206   The eelgrass biomass modelled from Eq. 6 explained 56% (R^2=0.56) of the total variation in the log-

207   transformed biomass observations without any systematic departures over the prediction range (Fig. 3). The

208   residual variation was considerable (Root MSE=0.6469 on the log-scale), corresponding to about ±90%

209   variation on individual observations. All parameter estimates were strongly significant (Table 2) and

210   importantly, the correlation between the parameter estimates of k_c and I_0/I_{sat} was small (r=0.1243). This

211   implied that the depth and cover terms of Eq. (6) were determined almost independently of each other. The

212   parameter estimate of k_c described that the eelgrass biomass reached a "saturation point" for eelgrass cover

213   around 54%. Similarly, the parameter estimate of I_0/I_{sat} suggested that light limitation became important at

214 depths where the surface irradiance was reduced to less than 30%. The monthly parameter estimates for B_{max}

215 displayed a significant (Wald test statistic=57.75; $p<0.0001$) and expected seasonal pattern increasing from

216 around 110-140 g DW m^{-2} in the spring months to a peak of 241 g DW m^{-2} in August and then declined

217 gradually in September and October to a level similar to that of June and July (~170 g DW m^{-2}; Fig. 4).

218 The residuals of biomass estimates from Eq. (6) followed the normal distribution closely and did not show

219 any systematic departures over the ranges of depth and cover (data not shown). However, the residuals

220 varied significantly among coastal sites ($F_{8,781}=14.15$; $p=<0.0001$). Accounting for site-specific differences

221 only reduced the remaining residual variation slightly (Root MSE=0.6038 on the log-scale), corresponding to

222 ±83% variation on individual observations. Thus, eelgrass biomass observations were quite variable with a

223 considerable amount of variation unaccounted for. Mean differences among coastal sites were between -0.26

224 and 0.33 on the log-scale (Table 3), corresponding to –23% and 39% deviation from the biomass-cover

225 relationship estimated over the entire data set. So in addition to the estimated relationship representing the

226 average across all coastal sites, there were site-specific characteristics yielding overall higher or lower

227 eelgrass biomass.

228 The marginal relationships between eelgrass biomass and depth (accounting for variations in cover, Secchi

229 depth, and month of sampling through the model) showed different decreases with depth among the coastal

230 sites, i.e. different "biomass attenuation" with depth (Fig. 5), which were caused by differences in light

231 attenuation among sites. In Køge Bugt and The Sound that had the highest water transparency (Table 1),

232 eelgrass biomass only decreased slightly between 0.7 and 7.8 m depth. Roskilde Fjord and Odense Fjord had

233 less clear waters and eelgrass biomass decreased already at depths >2 m (Fig. 5), although for Odense Fjord

234 this was only clear from the estimated relationship as eelgrass biomass was not sampled deeper than 3.2 m.

235 Differences between the estimated marginal relationships and observations, adjusted for variations in

236 eelgrass cover, interannual variation in Secchi depth and month of sampling, were large for Køge Bugt

237 (residuals 35% above the average) and The Sound (residual 21% below the average) (Fig. 5, Table 3). This

238 site-specific bias was smaller for Roskilde Fjord (-2%) and Odense Fjord (-11%).

239 Similarly, the marginal relationships showed a steep proportional increase in eelgrass biomass with eelgrass

240 cover in the range 0-20%, followed by a more gradual increase that almost flattened out when eelgrass cover

241 exceeded 40-50% (Fig. 6). The relationships for the different sites were quite similar, since site-specific

242 differences were based on the ratio between eelgrass sampling depth and Secchi depth ($\frac{z}{z_{SD}}$ in Eq. 6), that

243 exhibited small variations among sites (Table 1). As above, the relationship for Køge Bugt underestimated

244 eelgrass biomass observations, whereas the relationships for Roskilde Fjord, Odense Fjord and The Sound

245 overestimated biomass observations (cf. Table 3).

246 We calculated eelgrass biomass along four different transects where depth and eelgrass cover was monitored

247 as part of the national monitoring program (Fig. 7). All transects started at shallow depths and extended

248 beyond the eelgrass depth limits; however, depth did not increase continuously due to bottom topography.

249 Eelgrass biomass largely followed variations in eelgrass cover, displaying shifts between dense meadows

250 and bare sediments, but with relatively smaller biomass at deeper depths, which was most clearly seen in

251 Køge Bugt and Roskilde Fjord (Fig. 7a,c). Eelgrass biomass was predicted at 100-200 g DW m^{-2} in the dense

252 meadows, whereas the less dense patches had lower biomass.

253

254

255

DISCUSSION

257   We developed a general model that describes eelgrass biomass based on information on eelgrass cover for a

258   given depth and season and with associated information on water transparency of the coastal site. Hence, the

259   model allows a general conversion of eelgrass cover data to biomass. This model may constitute a useful tool

260   as information on eelgrass biomass is highly valuable for addressing functional aspects of eelgrass meadows

261   but sampling of biomass is destructive and costly while eelgrass cover is much easier and less costly to

262   assess on the large scale. As eelgrass biomass and cover at given depths are highly dependent on light

263   attenuation, the inclusion of a light attenuation term in the model enables a realistic fit to local light

264   conditions and makes the model generally applicable for areas showing seasonality of eelgrass biomass

265   similar to that of mid-latitude Danish coastal waters. The model also allows for converting aerial surveys of

266   eelgrass cover into biomass, provided that the bathymetry and Secchi depth of the area are known.

267   *Light regulation of eelgrass biomass*

268   The model provided estimates of the light level (I_0/I_{sat}) needed to support maximum eelgrass biomass, based

269   on the assumption that Secchi depths represent 20% of the surface irradiance (PAR). This assumption

270   corresponds to $K_d \cdot Z_{SD} = -\log(0.2) = 1.61$. Although this value corresponds to values reported for open

271   seawater (~1.5-1.7), $K_d \cdot z_{SD}$ is generally higher in estuaries and coastal waters (~1.9-3.9) influenced by

272   dissolved organic matter from land (Koenings and Edmundson 1991). The more recent monitoring

273   observations of the light attenuation coefficient suggest that $K_d \cdot z_{SD}$ ranges from 1.7 in Odense Fjord and

274   South Funen Archipelago to 2.1 in Roskilde Fjord (data not shown), corresponding to 12-18% of surface

275   irradiance at the Secchi depth. These values are higher than the value employed in the eelgrass biomass

276   model, but K_d and Z_{SD} are measured at deeper monitoring stations centrally located in the study sites,

277   whereas eelgrass biomass was sampled in shallower nearshore environments, where sediment resuspension is

278   more pronounced. Increased scattering from resuspended particles in the shallow environments reduces

279    $K_d \cdot z_{SD}$ (Gallegos et al. 2011), justifying the lower value applied in the model. Furthermore, eelgrass

280   biomass was sampled over a period (1990-2009) when nutrient inputs from Denmark were significantly

281   reduced (Carstensen et al. 2006), which also led to a decrease in the ratio between scattering and absorbance

282   (Pedersen et al. 2014). This suggests that $K_d \cdot z_{SD}$ has increased over time and therefore was lower during the

283   period of eelgrass biomass sampling, consistent with Pedersen et al. (2014) reporting an increase in $K_d \cdot z_{SD}$

284   in Roskilde Fjord from 1.8 (1985) to 2.2 (2008-2009). Unfortunately, light measurements within the eelgrass

285   meadows were not available, but $K_d \cdot z_{SD} = 1.61$ is not unrealistic given the arguments raised above.

286   The effect of light attenuation on eelgrass biomass was described as a biomass attenuation (Duarte 1991)

287   with depth, and Eq. (2) and the I_0/I_{sat}-value (Table 2) suggest that 73% of B_{max} can be obtained at 30% of the

288   surface irradiation, 55% of B_{max} can be obtained at 20% surface irradiation, and 30% of B_{max} can be obtained

289   at 10% surface irradiation. The nature of the light-dependency for eelgrass biomass is poorly documented in

290   the literature but our I_0/I_{sat} -value is possibly larger than the light level needed to support the depth limit of

291   eelgrass, for which there is considerable documentation. Based on laboratory studies Olesen (1996) found

292   that 11% of surface irradiance was needed to support eelgrass growth on an annual basis. Field studies have

293   reported somewhat higher light levels at the depth limit probably because loss of biomass due to other factors

294   than respiration contributes to defining the depth limit. Assuming 10% of the surface light at the Secchi

295   depth, Nielsen et al. (2002) showed that 18% surface irradiance was available at the depth limit of Danish

296   eelgrass meadows (Secchi depth ~4 m), while Krause-Jensen et al. (2011) found that 28% of surface

297   irradiance was available at the average depth limit of eelgrass in Danish coastal waters (Secchi depth

298   between 2.5 and 8 m). Combining these studies with the model results suggests that the eelgrass biomass at

299   the depth limit represents 50-70% of B_{max}. Obviously, the biomass attenuation component is not useful for

300   predicting depth limits (the biomass model is essentially unbounded towards deeper depths, cf. Eq. 2) and

301   depth limits are described through disappearance of eelgrass cover, as input to the model.

302   *Seasonal variation in biomass*

303   The increase in eelgrass biomass from May to August followed by a decline in September and October fits

304   well with the results from other studies at similar latitudes, which also show a biomass peak in

305   August/September (Sand-Jensen 1975; Olesen and Sand-Jensen 1994; Pedersen and Borum 1993; Clausen et

306   al. 2014). The increase in eelgrass biomass from May to August reflects the main growth season for eelgrass

307   with good light conditions and minimal physical exposure while the decline in biomass during autumn is a

308   combined effect from decreasing light levels and losses of leaves and shoots during autumn storms. The

309   timing of the biomass peak depends on latitude with earlier timing in the southern end of the distribution

310   range and later timing towards the Arctic (Clausen et al. 2014). Hence, the model would need adjustment of

311   the seasonal pattern if applied to eelgrass cover data from higher or lower latitudes.

312   The B_{max} estimate for August (Table 2) suggests a mean eelgrass biomass potential of 241 g DW m^{-2} for

313   100% eelgrass cover and no light limitation. This is consistent with Olesen and Sand-Jensen (1994), who

314   investigated a broad selection of 40 temperate eelgrass meadows and found an average aboveground biomass

315   of 245 g DW m^{-2} (10-90% percentile range: 111-391 g DW m^{-2}). Olesen and Sand-Jensen (1994) concluded

316   that the maximum attainable biomass of eelgrass meadows during midsummer was relatively uniform among

317   populations because self-shading within the stands sets an upper limit for biomass development. Probably for

318   the same reason maximum eelgrass biomass shows no significant change with latitude (Clausen et al. 2014).

319   The average increase in eelgrass biomass from May to August was 129 g DW m^{-2} and represented about a

320   doubling. Such marked seasonality from spring to summer is characteristic for eelgrass meadows (Olesen

321   and Sand-Jensen 1994; Duarte and Chiscano1999; Clausen et al. 2014). For example, Sand-Jensen (1975)

322   reported a quadrupling of the aboveground eelgrass biomass and a doubling of the belowground biomass

323   from March to August in a shallow Danish embayment, paralleling a total production of about 1100 g DW

324   m^{-2} from April to October.

325   *Spatial variation and applicability of the model*

326   The estimated model translates eelgrass cover and depth into eelgrass biomass, provided that the Secchi

327   depth is also known. Analysis of the residuals suggests that the model could introduce a substantial bias (-

328   23%-39%, Table 3) in such biomass estimates, but this bias may also result from other factors (input data)

329   than model bias. As discussed above, Secchi depth was monitored at deeper stations for all sites and this may

330   introduce a bias, because these data represent light conditions in the eelgrass meadows with varying degree

331   of bias. Differences among areas in $K_d \cdot z_{SD}$ for converting Secchi depths to light attenuation may also

332   introduce a bias, and it is therefore better to use Eq. (3) for the light attenuation, if K_d is measured.

333   Variation among sites in the biomass-cover relationship was observed (Table 3). It cannot be excluded that

334   differences between observers and slight differences in methods explain part of this variation as many divers

335   contributed to the survey. If differences between observers could be ignored, site-specific variation in the

336   biomass for a given cover likely reflects differences between sites in loss factors and/or growth conditions

337   unrelated to light-attenuation in the water column (which the model accounts for). One such loss factor could

338   be grazing, e.g. by water fowl, which would affect biomass without necessarily affecting cover and therefore

339   would result in the model overestimating the actual biomass at such sites. Drifting algae, which tend to

340   accumulate in eelgrass beds (Rasmussen et al. 2013, 2015) might also reduce the aboveground biomass

341   without affecting cover and might be part of the explanation why the model overestimates the eelgrass

342   biomass at sites such as Køge Bugt and Kertinge Nor, which have been known for large occurrences of

343   drifting filamentous brown algae during the study period (Riisgård et al. 1995). By contrast, well-established

344   and dense eelgrass meadows tend to facilitate their own growth and resilience through positive feed–backs,

345   which may involve more efficient light utilization in the closed canopy, increased sedimentation and

346   improved recycling of nutrients as well as increased top-down control of epiphytic algae on leaf surfaces

347   (Gutierrez et al. 2011; Sand-Jensen et al. 2007; van der Heide et al. 2011) and may thereby maintain a larger

348   biomass at a given cover. Such positive feed-backs could explain why the model underestimated the biomass

349   at the South Funen Archipelago and The Sound, known for their well-developed eelgrass meadows (Krause-

350   Jensen et al. 2000).

351   The perspective is to employ the model to scale-up eelgrass cover estimates for an entire coastal ecosystem

352   to calculate nutrient and carbon budgets for eelgrass, and to compare these to similar budgets for the water

353   column and other biological components (Neckles et al. 2012). This will allow to quantitatively assess the

354   role of eelgrass in the biogeochemical cycling of elements in coastal ecosystems.

15

364

References

Carstensen, J., D.J. Conley, J.H. Andersen and G. Ærtebjerg. 2006. Coastal eutrophication and trend
reversal: A Danish case study. Limnology & Oceanography 51: 398−408.

Carstensen, J. 2010. Censored data regression: statistical methods for analyzing Secchi transparency in
shallow systems. Limnology & Oceanography: Methods 8: 376–385.

Cebrián, J., C.M. Duarte, N. Marbà and S. Enriquez. 1997. Magnitude and fate of the production of four co-
occurring western Mediterranean seagrass species. Marine Ecology Progress Series 155: 29−44.

Clausen, K.K., P. Clausen, C.C. Faelled and K.N. Mouritsen. 2012. Energetic consequences of a major
change in habitat use: endangered Brent geese *Branta bernicla hrota* losing their main food resource. Ibis
154: 803−814.

Clausen, K.K., D. Krause-Jensen, B. Olesen and N. Marbà. 2014. Seasonality of eelgrass biomass across
gradients in temperature and latitude. Marine Ecology Progress Series 506: 71−85.

Duarte, C.M. 1991. Seagrass depth limits. Aquatic Botany 40: 363–377.

Duarte, C.M. and C.L. Chiscano. 1999. Seagrass biomass and production: a reassessment. Aquatic Botany
65: 159–174.

Duarte, C.M., N. Marbà, D. Krause-Jensen and M. Sánchez-Camacho. 2007. Testing the predictive power of
seagrass depth limit models. Estuaries and Coasts 30: 652–656.

Duarte, C.M., I.J. Losada, I.E. Hendriks, I. Mazarrasa and N. Marbà. 2013. The role of coastal plant
communities for climate change mitigation and adaptation. Nature Climate Change 3: 961–968.

Fourqurean, J.W., C.M. Duarte, H. Kennedy, N. Marbà, M. Holmer, M.A. Mateo, E.T. Apostolaki, G.A.
Kendrick, D. Krause-Jensen, K.J. McGlathery and O. Serrano. 2012. Seagrass ecosystems as a globally
significant carbon stock. Nature Geoscience 5: 505–509.

Gallegos, C.L., P.J. Werdell, and C.R. McClain. 2011. Long-term changes in light scattering in Chesapeake
Bay inferred from Secchi depth, light attenuation, and remote sensing measurements. Journal of
Geophysical Research 116: C00H08. doi:10.1029/2011JC007160.

390 Gutiérrez, J.L., C.G. Jones, J.E. Byers, K.K. Arkema, K. Berkenbusch, J.A. Commito, C.M. Duarte, S.D.

391   Hacker, J.G. Lambrinos, I.E. Hendriks, P.J. Hogarth, M.G. Palomo and C. Wild. 2011. Physical

392   ecosystem engineers and the functioning of estuaries and coasts. Treatise on Estuarine and Coastal

393   Science 7: 53–81.

394 Hemminga, M.A. and C.M. Duarte. 2000. Seagrass ecology. Cambridge University Press, Cambridge.

395 Koch, E.M. 2001. Beyond light: physical, geological, and geochemical parameters as possible submersed

396   aquatic vegetation habitat requirements. Estuaries 24: 1–17.

397 Koenings, J.P. and J.A. Edmundson. 1991. Secchi disk and photometer estimates of light regimes in

398   Alaskan lakes—effects of yellow color and turbidity. Limnology & Oceanography 36: 91–105.

399 Krause-Jensen, D., A.L. Middelboe, K. Sand-Jensen and P.B. Christensen. 2000. Eelgrass, *Zostera marina*,

400   growth along depth gradients: Upper boundaries of the variation as a powerful predictive tool. Oikos 91:

401   233–244.

402 Krause-Jensen, D., M.F. Pedersen and C. Jensen. 2003. Regulation of eelgrass *(Zostera marina)* cover

403   along depth gradients in Danish coastal waters. Estuaries 26: 866–877.

404 Krause-Jensen, D., J. Carstensen, S.L. Nielsen, T. Dalsgaard, P.B. Christensen, H. Fossing and M.B.

405   Rasmussen. 2011. Sea bottom characteristics affect depth limits of eelgrass *Zostera marina*. Marine

406   Ecology Progress Series 425: 91–102.

407 Marbá, N, D. Krause-Jensen, T. Alcoverro, S. Birk, A. Pedersen, J.M. Neto, S. Orfanidis, J.M. Garmendia, I.

408   Muxika, A. Borja, K. Dencheva and C.M. Duarte. 2013. Diversity of European seagrass indicators -

409   Patterns within and across regions. Hydrobiologia 704: 265–278. DOI 10.1007/s10750-012-1403-7.

410 McGlathery, K.J., L.K. Reynolds, L.W. Cole, R.J. Orth, S.R. Marion and A. Schwarzschild. 2012. Recovery

411   trajectories during state change from bare sediment to eelgrass dominance. Marine Ecology Progress

412   Series 448: 209–221.

413 Neckles, H.A., B.S. Kopp, B.J. Peterson and P.S. Pooler. 2012. Integrating scales of seagrass monitoring to

414   meet conservation needs. Estuaries and Coasts 35: 23–46. DOI 10.1007/s12237-011-9410-x.

415 Nielsen, S.L., K. Sand-Jensen, J. Borum and O. Geertz-Hansen. 2002. Depth colonization of eelgrass

416 (*Zostera marina*) and macroalgaeas determined by water transparency in Danish coastal waters. Estuaries

417 25: 1025–1032.

418 Olesen, B. 1996. Regulation of light attenuation and eelgrass *Zostera marina* depth distribution in a Danish

419 embayment. Marine Ecology Progress Series 134: 187–194.

420 Olesen, B. and K. Sand-Jensen. 1994. Biomass-density patterns in the temperate seagrass *Zostera marina*.

421 Marine Ecology Progress Series 109: 283–291.

422 Pedersen, M.F. and J. Borum. 1993. An annual nitrogen budget for a seagrass *Zostera marina* population.

423 Marine Ecology Progress Series 101: 169–169.

424 Pedersen, T.M., K. Sand-Jensen, S. Markager and S.L. Nielsen. 2014. Optical changes in a eutrophic estuary

425 during reduced nutrient loadings. Estuaries and Coasts 37: 880–892. DOI 10.1007/s12237-013-9732-y

426 Platt, T., A.D. Jassby. 1976. The relationship between photosynthesis and light for natural assemblages of

427 coastal marine phytoplankton. Journal of Phycology 12: 421–430.

428 Plummer, M.L., C.J. Harvey, L.E. Anderson, A.D. Guerry and M.H. Ruckelshaus. 2013. The role of eelgrass

429 in marine community interactions and ecosystem services: Results from ecosystem-scale food web

430 models. Ecosystems 16: 237–251. DOI: 10.1007/s10021-012-9609-0.

431 Rasmussen, J.R., M.F. Pedersen, B. Olesen, S.L. Nielsen and T.M. Pedersen. 2013. Temporal and spatial

432 dynamics of ephemeral drift-algae in eelgrass, *Zostera marina*, beds. Estuarine Coastal Shelf Science

433 119: 167–175.

434 Rasmussen, J.R., K. Dromph, C. Göke and D. Krause-Jensen. 2015. Reduced cover of drifting macroalgae

435 following nutrient reduction in Danish coastal waters. Estuaries and Coasts. DOI 10.1007/s12237-014-

436 9904-4.

437 Riisgård, H.U., P.B. Christensen, N.J. Olesen, J.K. Petersen, M.M. Møller and P. Andersen. 1995. Biological

438 structure in a shallow cove (Kertinge Nor, Denmark) – control by benthic nutrient fluxes and suspension-

439 feeding ascidians and jellyfish. Ophelia 41: 329–344.

440 Sand-Jensen K. 1975. Biomass, net production and growth dynamics in an eelgrass (*Zostera marina L.*)

441 population in Vellerup Vig. Denmark. Ophelia 14: 185–201.

442 Sand-Jensen, K., J. Borum. 1991. Interactions among phytoplankton, periphyton, and macrophytes in

443   temperate freshwaters and estuaries. Aquatic Botany 41, 137–175.

444 Sand-Jensen, K., T. Binzer and A.L. Middelboe. 2007. Scaling of photosynthetic production of aquatic

445   macrophytes - a review. Oikos 116: 280–294, doi: 10.1111/j.2006.0030-1299.15093.x.

446 van der Heide, T., E.H. van Nes, M.M. van Katwijk, H. Olff and A.J.P. Smolders. 2011. Positive feedbacks

447   in seagrass ecosystems – Evidence from large-scale empirical data. PLoS ONE 6(1): e16504.

448   doi:10.1371/journal.pone.0016504.

449

Table 1 Overview of data sets used for estimating the eelgrass aboveground biomass-cover relationship. For each coastal site is listed the number of observations, distributed over number of years, number of transects and the specific months sampled (by month number, i.e. 3=March, 4=April, etc.). Means and ranges for the variables used in the relationship are shown. Annual means (March-September) of Secchi depth were used and no range is given for sites with a single sampling year.
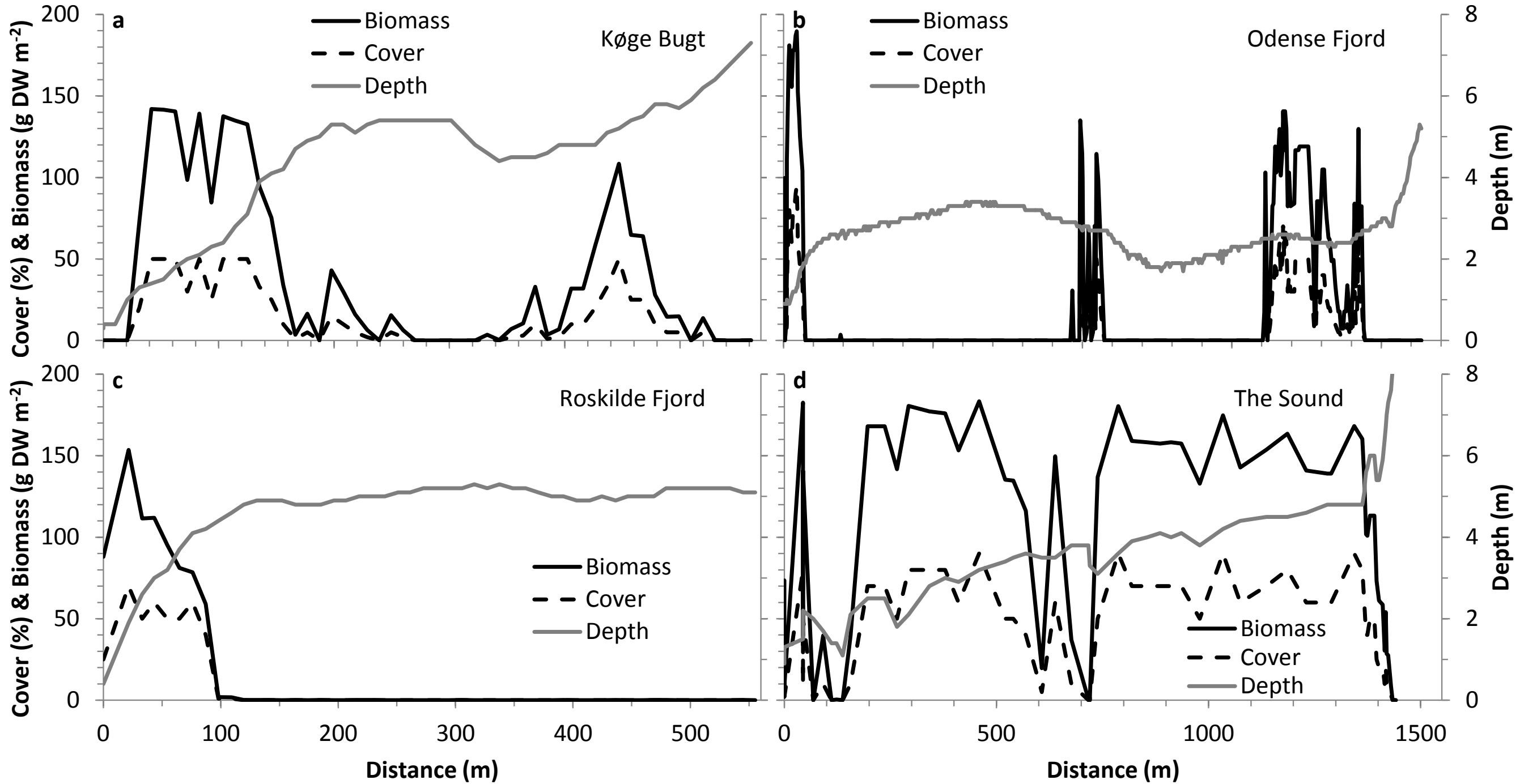
Coastal site	# of years	Months sampled	# of transects	# of obs.	Secchi depth (m)		Transect depth (m)		Cover (%)		Biomass (g DW m^{-2})	
					Mean	Range	Mean	Range	Mean	Range	Mean	Range
Flensborg Fjord	7	3-6, 8-9	1	83	5.0	4.4-5.4	2.8	1.0-5.0	66	1-100	148	2.8-546
Helnæs Bugt	1	9	7	38	5.6		1.5	0.7-2.5	72	50-95	176	64-312
Kertinge Nor	1	9	4	12	2.2		2.0	0.7-2.5	100	100	122	31-240
Køge Bugt	6	4-10	4	156	7.1	6.6-7.5	4.3	0.7-7.8	45	1-100	113	0.2-573
Odense Fjord	3	5-6, 8-10	3	120	3.2	2.8-3.5	1.6	0.8-3.2	81	20-100	128	5.0-388
Roskilde Fjord	6	3-8	10	105	3.9	2.7-4.5	2.4	1.0-6.0	46	2-100	113	2.9-399
South Funen Archipelago	1	9	2	24	6.5		3.7	2.6-5.2	93	75-100	91	34-178
The Sound	10	5-9	11	253	7.8	7.4-8.7	3.3	1.0-6.3	86	10-100	155	3.9-511

Table 2 Parameter estimates obtained from Eq. (6) using 791 eelgrass biomass observations (log-transformed). SE=standard error of the parameter estimate.
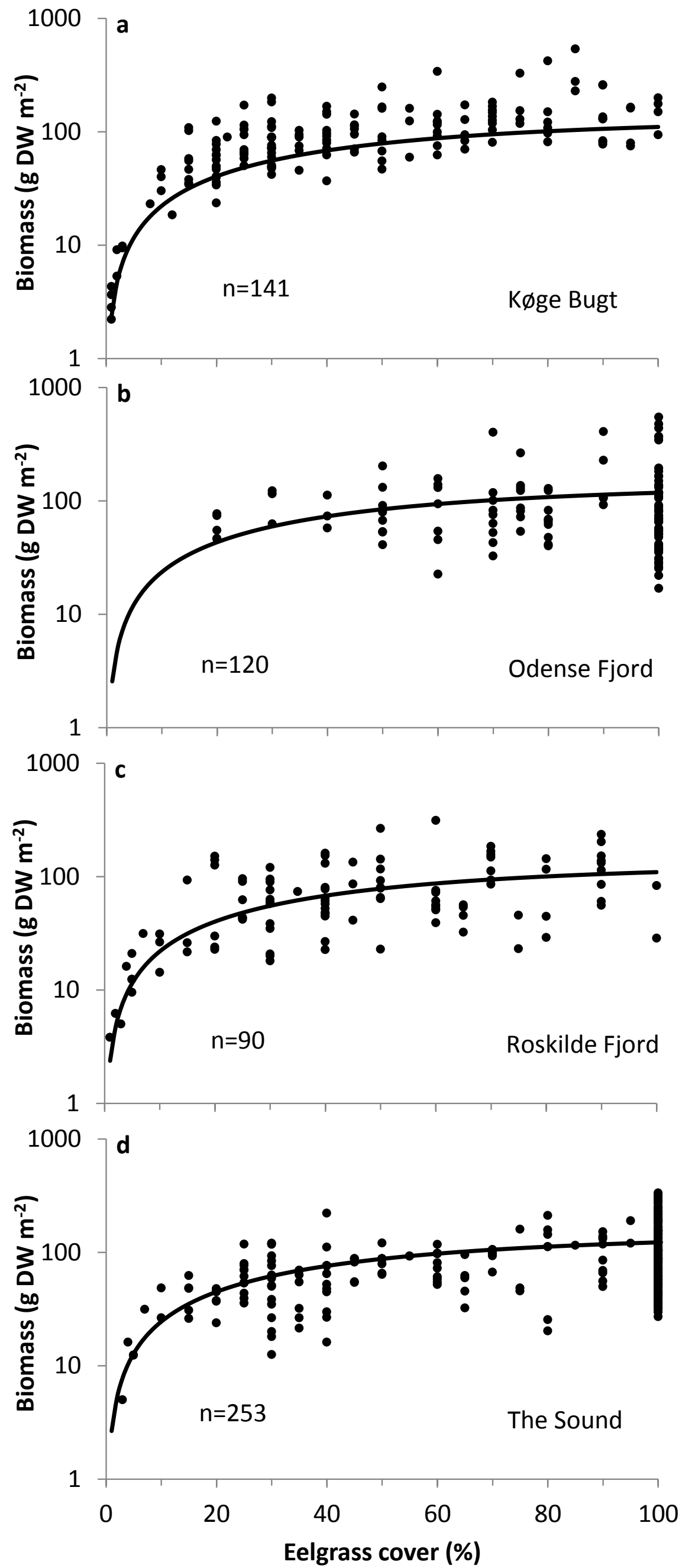
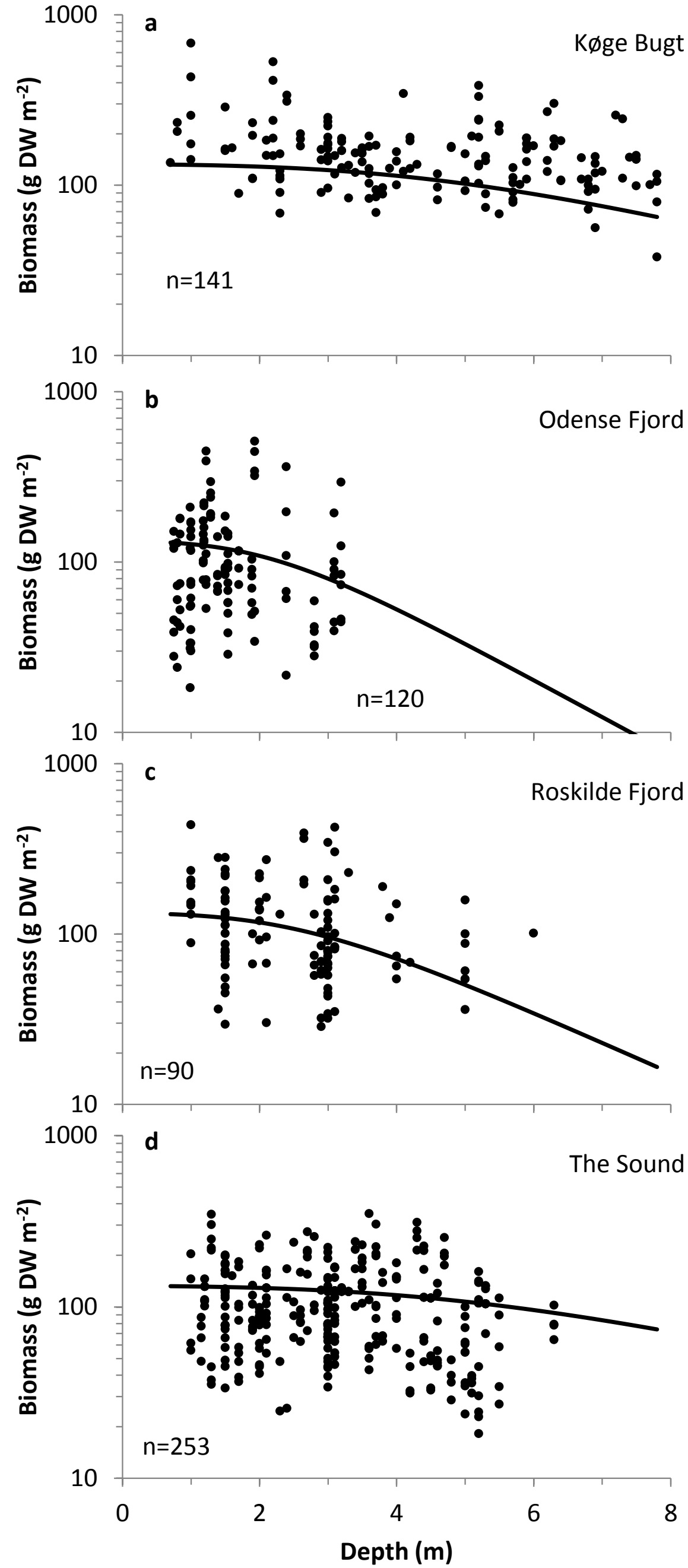| Parameter	Estimate	SE	t-test	Probability
k_c	54.26	7.82	6.94	<.0001
I_0/I_{sat}	3.12	0.38	8.28	<.0001
$\log(B_{max})$ (Mar)	4.79	0.15	32.04	<.0001
$\log(B_{max})$ (Apr)	4.93	0.16	30.33	<.0001
$\log(B_{max})$ (May)	4.72	0.13	35.06	<.0001
$\log(B_{max})$ (Jun)	5.16	0.12	44.50	<.0001
$\log(B_{max})$ (Jul)	5.13	0.12	44.01	<.0001
$\log(B_{max})$ (Aug)	5.48	0.08	65.91	<.0001
$\log(B_{max})$ (Sep)	5.12	0.10	52.79	<.0001
$\log(B_{max})$ (Oct)	5.20	0.12	42.67	<.0001

Table 3 Residual variation from estimating Eq. (6) among coastal sites. For each coastal site is listed the mean of the residuals, the standard error of the mean (SE), the *t*-statistic for testing if the mean equals zero and its associated probability.
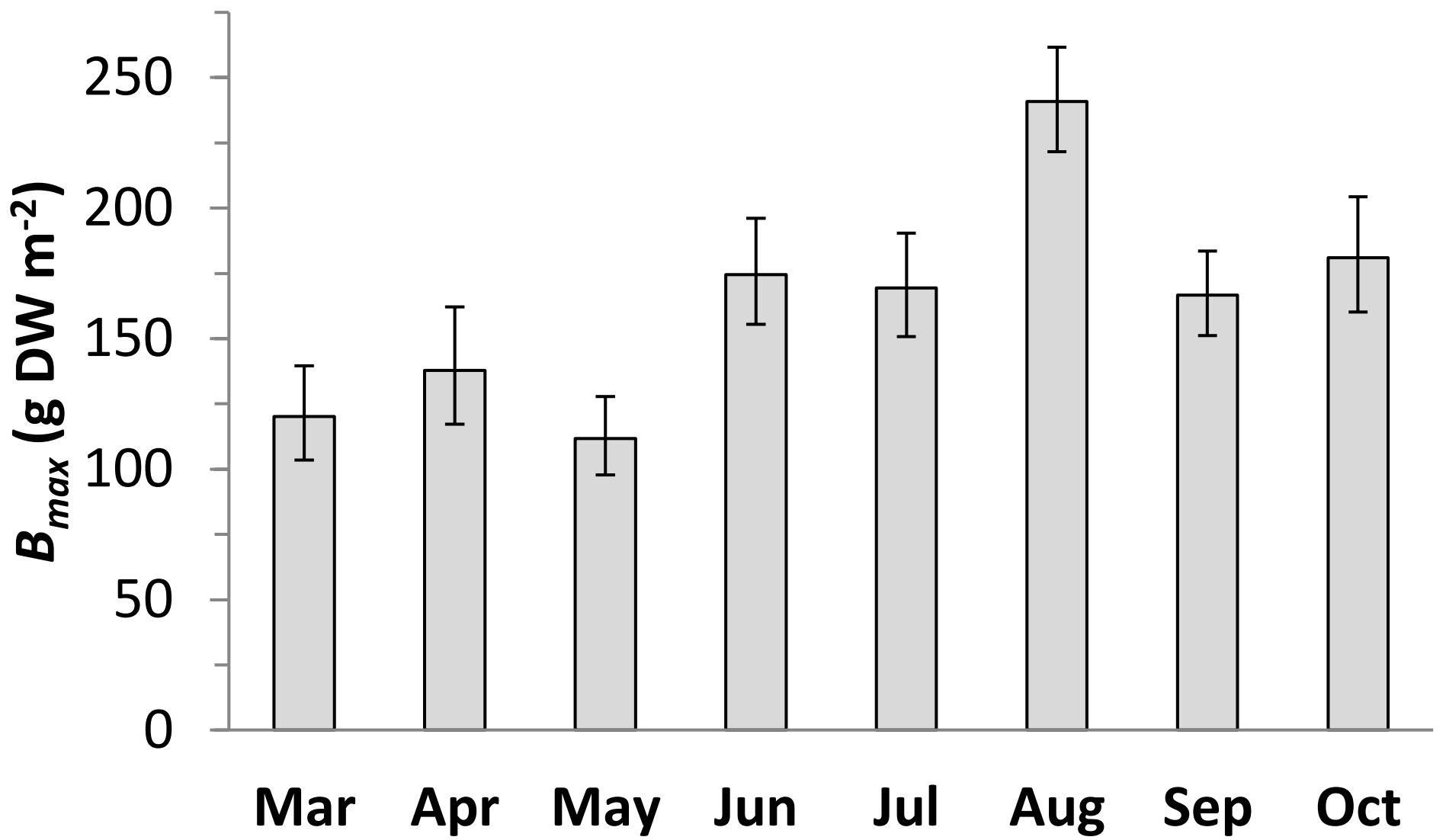
Coastal site	Mean	SE	*t*	*p*
Flensborg Fjord	0.256	0.067	3.82	0.0001
Helnæs Bugt	0.332	0.098	3.38	0.0007
Kertinge Nor	0.190	0.174	1.09	0.2770
Køge Bugt	0.298	0.048	6.16	<0.0001
Odense Fjord	-0.117	0.055	-2.13	0.0335
Roskilde Fjord	-0.016	0.059	-0.28	0.7823
South Funen Archipelago	-0.258	0.123	-2.10	0.0363
The Sound	-0.237	0.038	-6.25	<0.0001

a

Biomass (g DW m^{-2})

n=141

Køge Bugt

b

Biomass (g DW m^{-2})

n=120

Odense Fjord

c

Biomass (g DW m^{-2})

n=90

Roskilde Fjord

d

Biomass (g DW m^{-2})

n=253

The Sound

Eelgrass cover (%)

a Køge Bugt

n=141

b Odense Fjord

n=120

c Roskilde Fjord

n=90

d The Sound

n=253

Biomass (g DW m^{-2})

Depth (m)

a

Biomass (g DW m⁻²)

<2 m

b

Biomass (g DW m⁻²)

2-4 m

c

Biomass (g DW m⁻²)

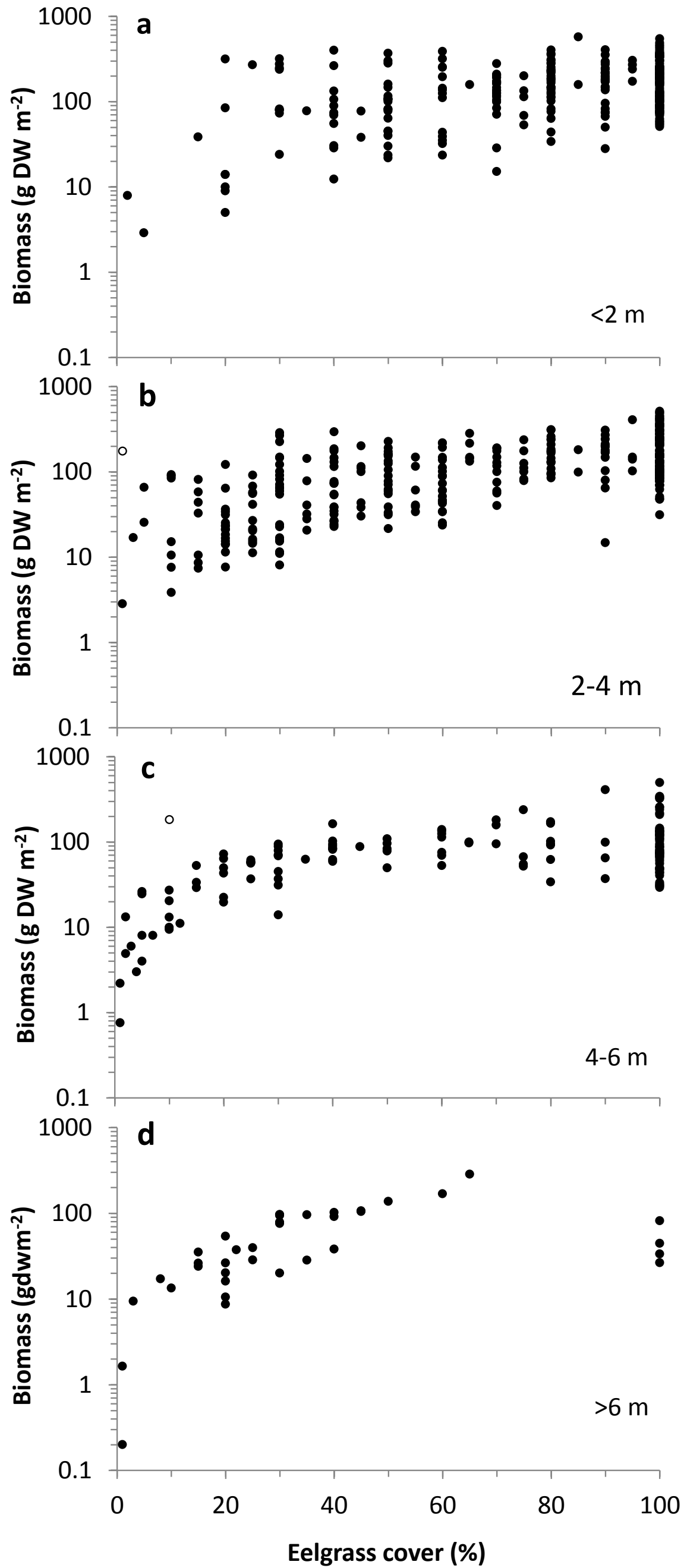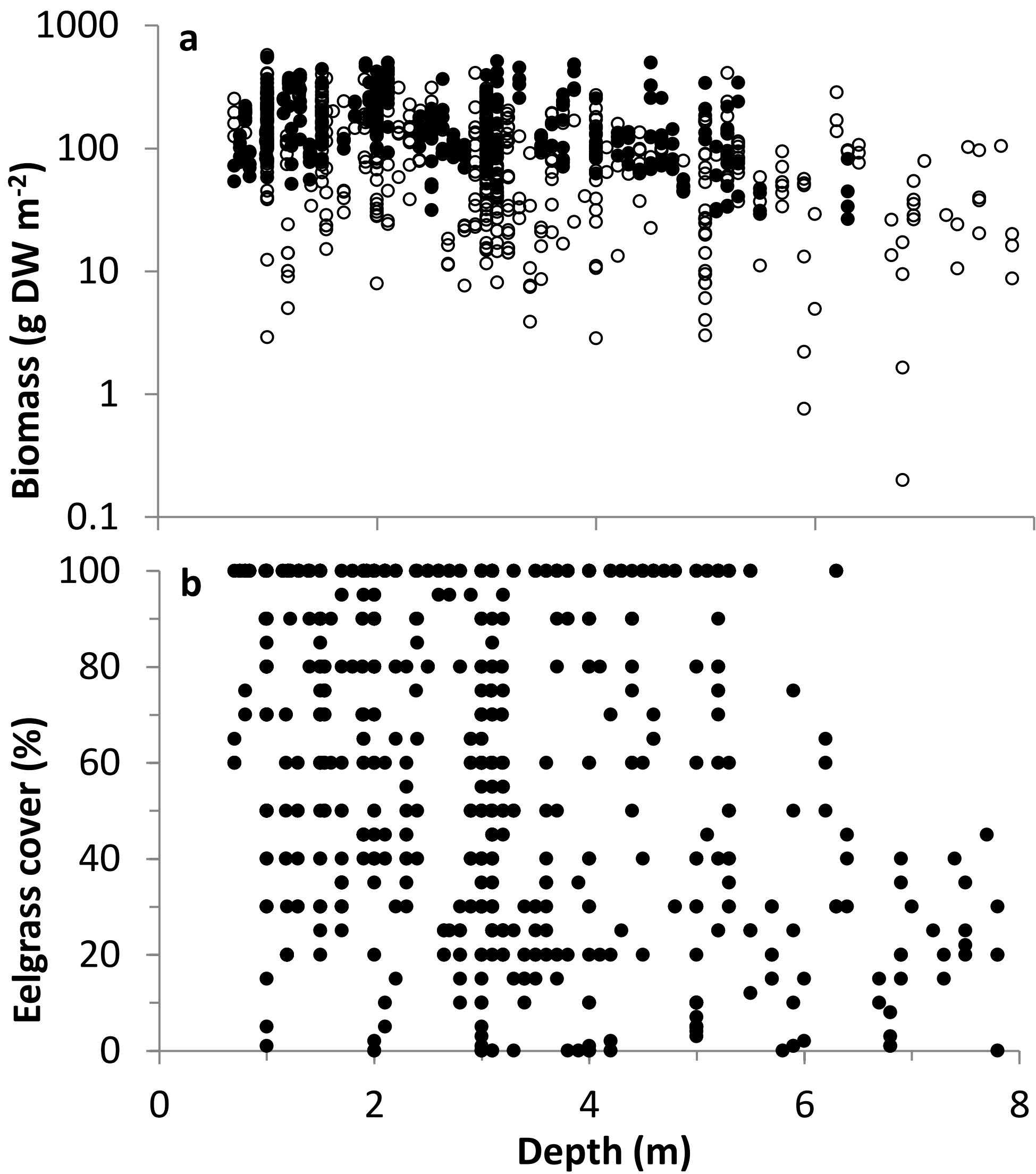4-6 m

d

Biomass (gdwm⁻²)

>6 m
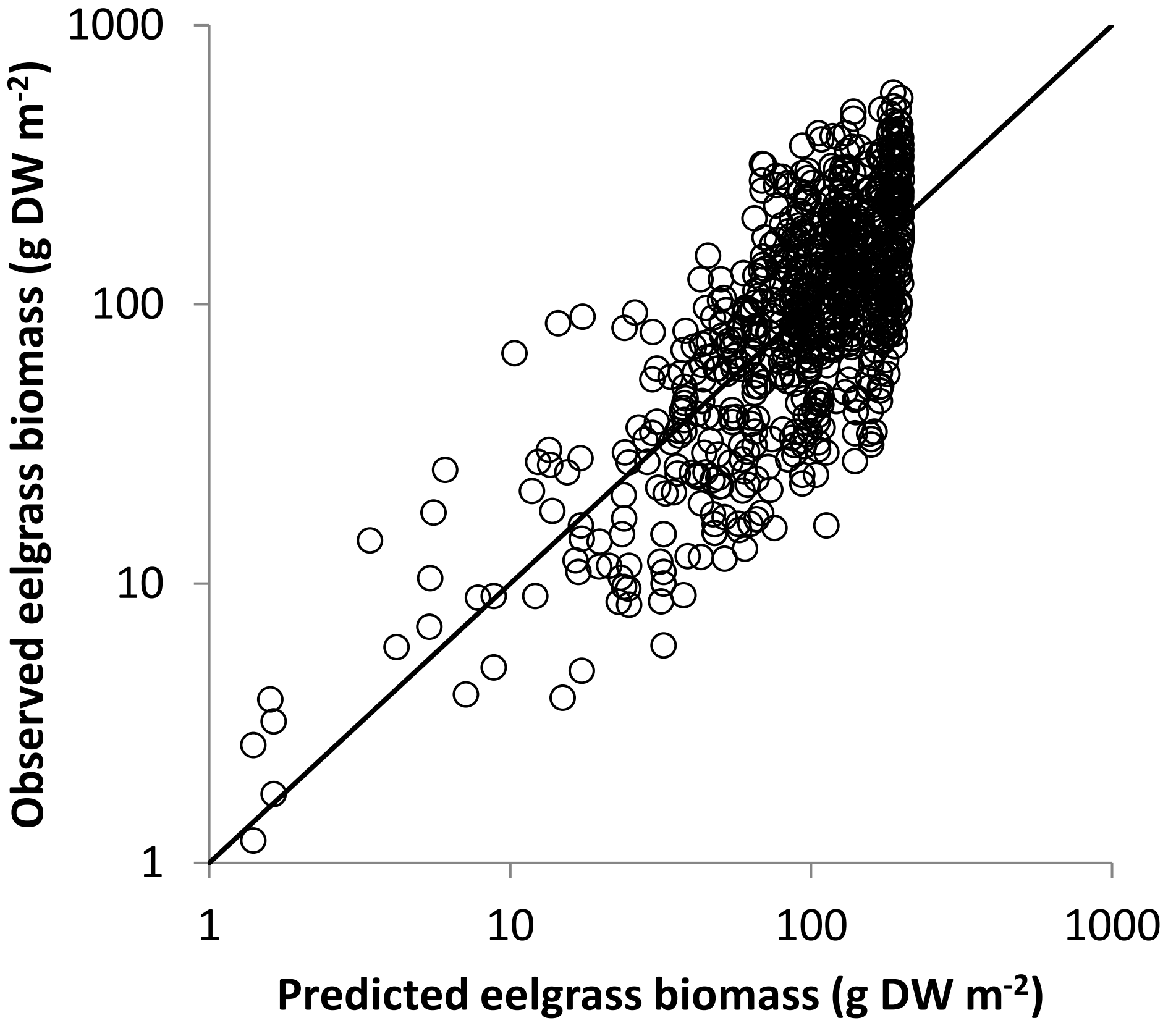
Eelgrass cover (%)

FIGURE LEGENDS

Fig. 1 Eelgrass aboveground biomass (**a**) and eelgrass cover (**b**) versus depth shown for all 791 samples. a) closed symbols are observations with 100% cover and open symbols have less than 100% eelgrass cover

Fig. 2 Eelgrass aboveground biomass versus cover shown for different depth. **a:** 0.5-2 m, **b:** 2-4 m, **c:** 4-6 m, **d:** 6-8 m. Two outliers are shown with open symbols

Fig. 3 Predicted versus observed eelgrass aboveground biomass.

Fig. 4 Monthly estimates of maximum aboveground eelgrass biomass at 100% cover (B_{max}). Estimates were obtained from back-transforming the estimates in Table 2. Error bars show the standard errors of the monthly estimates

Fig. 5 Marginal relationships between aboveground eelgrass biomass and depth for four selected sites. Variations in eelgrass cover, interannual variations in Secchi depth and month of sampling were accounted for by adjusting observations (dots) and the modeled relationships (solid line) to a common eelgrass cover of 100% and an average over all months from March to October using the estimated relationship (Eq. 6) and annual means of Secchi depth. The four selected sites had the most biomass observations and a broad span in Secchi depths and eelgrass depth ranges (Table 1)

Fig. 6 Marginal relationships between aboveground eelgrass biomass and cover for four selected sites. Variations in sampling depth, interannual variations in Secchi depth and month were accounted for by adjusting observations (dots) and the modeled relationships (solid line) to a mean sampling depth (Table 1) and an average over all months from March to October using the estimated relationship (Eq. 6) and annual means of Secchi depth. The four selected sites had the most biomass observations and a broad span in Secchi depths and eelgrass depth ranges (Table 1)

Fig. 7 Application of the estimated eelgrass biomass vs. cover relationship to four transects from selected sites monitored in 2013. Depth and eelgrass cover are measured along transects of variable length and

converted to eelgrass biomass using Eq. (6). Secchi depths used in the equations were 7.2 m (Køge Bugt),

4.1 m (Odense Fjord), 3.7 m (Roskilde Fjord), and 8.9 m (The Sound)
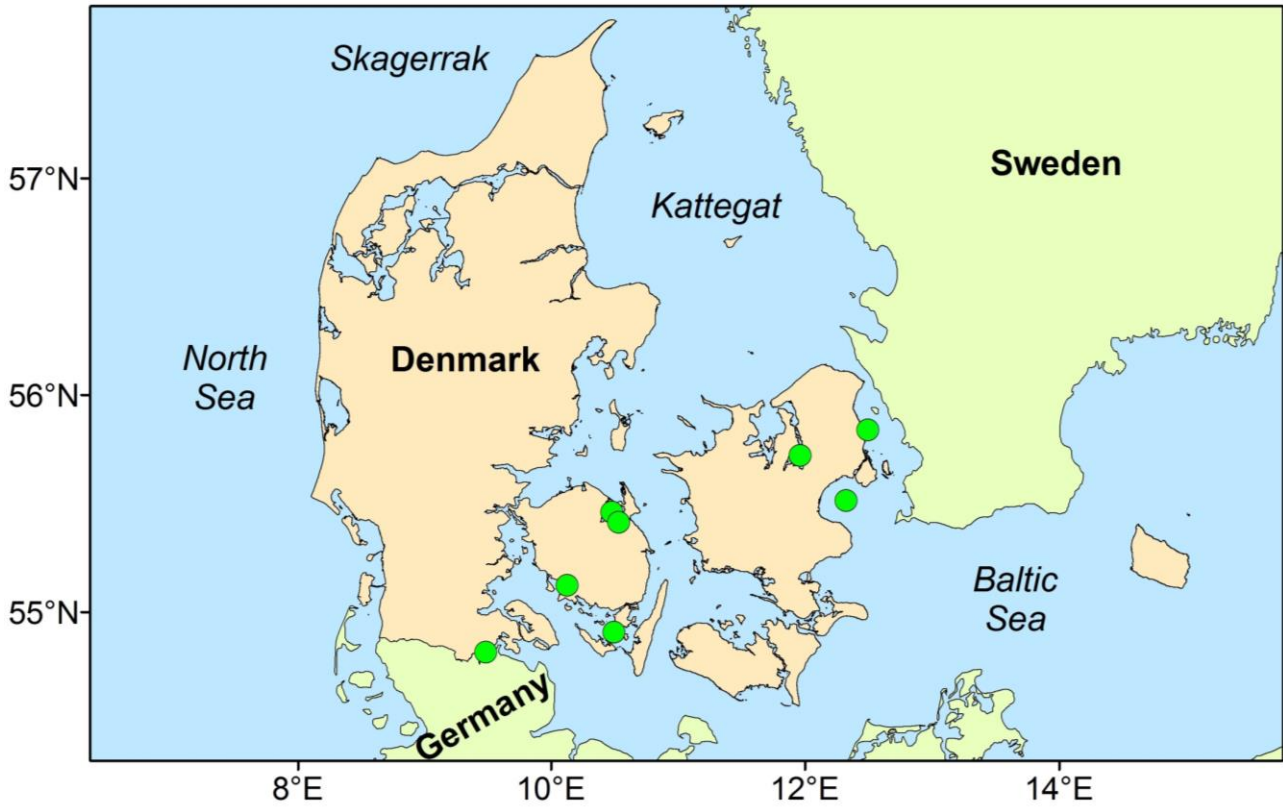
Supplementary information

Fig. S1: Location of coastal sites where eelgrass biomass was sampled.